Structure

Volume 21
Number 11
November 5, 2013
www.cellpress.com

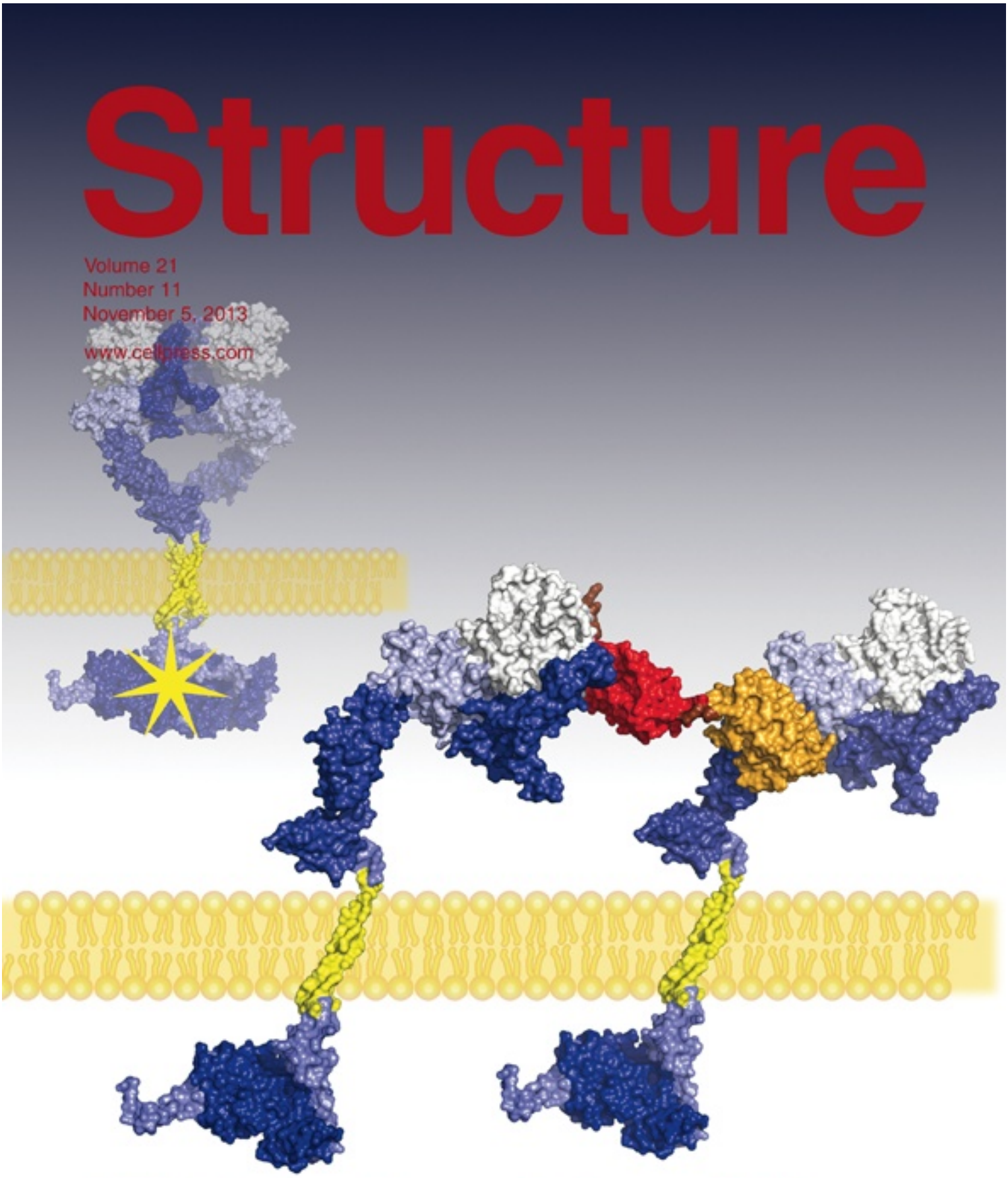

HER2: A New Approach for an Old Target

Structure
Article

Structural Basis for Eliciting a Cytotoxic Effect in HER2-Overexpressing Cancer Cells via Binding to the Extracellular Domain of HER2

Christian Jost,[1] Johannes Schilling,[1] Rastislav Tamaskovic,[1] Martin Schwill,[1] Annemarie Honegger,[1] and Andreas Plückthun[1,*]
[1]Department of Biochemistry, University of Zürich, 8057 Zürich, Switzerland
*Correspondence: plueckthun@bioc.uzh.ch
http://dx.doi.org/10.1016/j.str.2013.08.020

SUMMARY

Human epidermal growth factor receptor-2 (HER2) is a receptor tyrosine kinase directly linked to the growth of malignancies from various origins and a validated target for monoclonal antibodies and kinase inhibitors. Utilizing a new approach with designed ankyrin repeat proteins (DARPins) as alternative binders, we show that binding of two DARPins connected by a short linker, one targeting extracellular subdomain I and the other subdomain IV, causes much stronger cytotoxic effects on the HER2-addicted breast cancer cell line BT474, surpassing the therapeutic antibody trastuzumab. We determined crystal structures of these DARPins in complex with the respective subdomains. Detailed models of the full-length receptor, constrained by its rigid domain structures and its membrane anchoring, explain how the bispecific DARPins connect two membrane-bound HER2 molecules, distorting them such that they cannot form signaling-competent dimers with any EGFR family member, preventing any kinase dimerization, and thus leading to a complete loss of signaling.

INTRODUCTION

The human epidermal growth factor receptor 2 (HER2, hErbB2) is a receptor tyrosine kinase expressed on the cell surface of nearly every cell in the human body. HER2 contributes to multiple signal transduction pathways, but mainly stimulates the HER3/PI3K/Akt pathway and the mitogen-activated protein (MAP) kinase cascades, leading to cell survival and proliferation (Yarden and Sliwkowski, 2001; Craven et al., 2003). HER2 amplification promotes tumorigenesis (Faber et al., 2010), and human tumors and various tumor cell lines rely on HER2 signaling for their survival. Such cancer cells are often referred to as "HER2-addicted" (Moasser, 2007).

Trastuzumab (Herceptin, Genentech), a humanized monoclonal antibody binding to the extracellular subdomain IV of HER2 (HER2_IV), is effectively used in the clinic to treat patients with HER2-overexpressing breast cancers (Cobleigh et al., 1999; Finn and Slamon, 2003). Besides exerting cytotoxic effects in vivo through antibody-dependent cellular cytotoxicity (ADCC) and complement-dependent cytotoxicity (CDC), trastuzumab mainly acts as a cytostatic agent inducing a G1 phase cell-cycle arrest in HER2-amplified cancer cells (Sliwkowski et al., 1999). Inhibition of HER2 homodimerization (Ghosh et al., 2011) and of HER2/HER3 heterodimerization (Junttila et al., 2009) is thought to be responsible for this antiproliferative effect. Pertuzumab (Perjeta, Genentech), a humanized monoclonal antibody binding next to the dimerization arm on subdomain II of HER2, shows only moderate antitumor effects in vitro on HER2-overexpressing breast cancer cell lines (shown for SkBr-3 cells; Schaefer et al., 1997). However, for cell lines with normal HER2 expression levels that are grown in the presence of the HER3-activating ligand Heregulin, which efficiently stimulates HER2/HER3 heterodimer formation (Sliwkowski et al., 1994), the effect of pertuzumab exceeds the effect of trastuzumab (Schaefer et al., 1997). This finding can be explained in that pertuzumab, bound next to the HER2 dimerization arm, sterically blocks the formation of back-to-back heterodimers that are induced by ligand stimulation of HER3 (Franklin et al., 2004).

Recently, Trastuzumab emtansine (T-DM1) (Kadcyla), a maytansinoid conjugate (Burris et al., 2011; Verma et al., 2012), has become Food and Drug Administration approved. It is thought to be endocytosed with the slow internalization and recycling rates intrinsic to ErbB2 and thus to release the toxin. These encouraging data stimulate the search for novel mechanisms of action, which may pave the way for agents not requiring a conjugated toxin.

Recent studies on the regulation of the homologous receptor EGFR have shown that receptor dimerization is required, but may not be sufficient for full receptor activation (Arkhipov et al., 2013; Endres et al., 2013). Dimerization of ECD, transmembrane (TM) helices and, as a consequence, the kinase domains have to take place in a well-ordered mechanism, requiring, for example, pairing the N-terminal, but not the C-terminal, parts of the two TM-helices for functional dimerization of the kinase domains. Additional factors modifying the coupling between dimerization of the extracellular domain to the dimerization and activation of the kinase domain may contribute to the subtle regulation of receptor activity (Arkhipov et al., 2013; Endres et al., 2013).

Tumor cells becoming refractory to trastuzumab treatment present a major clinical problem. This is caused not only by

downregulation or loss of HER2 expression, but also by various mutations bypassing the blocked HER2-signaling, including constitutive activation of the PI3K-signaling pathway, accumulation of a constitutively active HER2-kinase, and crosstalk of HER2 with other growth factor receptors (Xia et al., 2004; Sergina et al., 2007). Acquisition of trastuzumab resistance might be promoted by the cytostatic effect of trastuzumab, which allows the tumor to undergo a directed evolution to escape treatment. Thus, an optimal drug against HER2-overexpressing cancer cells would have to be cytotoxic instead of cytostatic, but the cytotoxicity should not broadly aim at all HER2-expressing cells, but rather specifically target cancer cells that are dependent on HER2.

The concept that HER2 remains the active oncogenic driver in many cancer cells (e.g., by signaling through HER2-HER3-heterodimers) motivates further research for alternative molecular therapies targeting HER2 (Gajria and Chandarlapaty, 2011). To expand and complement existing anti-HER2 therapies beyond pertuzumab and trastuzumab or any toxin conjugates, such as T-DM1 (Burris et al., 2011), further HER2 binders that employ alternative mechanisms should thus be developed for abolishing HER2-dependent signaling.

Designed ankyrin repeat proteins (DARPins) are binding scaffolds that have recently been developed to expand the range of formats and applications beyond what is possible with immunoglobulin-based proteins (Binz et al., 2004; Boersma and Plückthun, 2011). Because of their small size, high stability, and efficient folding, DARPins can easily be fused to each other in different orientation and geometries and to different protein domains to generate multivalent or multispecific constructs or to provide targeting specificity to effector proteins. They are highly suitable for site-specific chemical modification (Simon et al., 2012), such as coupling to polyethylene glycol (PEGylation) to increase the hydrodynamic radius and thus serum half-life and thereby promote tumor uptake (Zahnd et al., 2010) or conjugation of toxins. While they have been used for targeting toxins to a tumor (Martin-Killias et al., 2011), it is of interest to investigate whether they can also exert a biological function by themselves. Thus, they appear predestined as binding moieties for novel approaches in targeted therapy. DARPins recognizing the soluble recombinant ectodomain of HER2 (HER2-ECD) with subnanomolar to low-nanomolar affinities were selected by ribosome display (Zahnd et al., 2007) and phage display (Steiner et al., 2008). These HER2-specific DARPins have been used for histochemical staining (Theurillat et al., 2010), for tumor targeting of toxins (Zahnd et al., 2010), and for targeting adenoviral (Dreier et al., 2013) and lentiviral vectors (Münch et al., 2011) to HER2-overexpressing cells.

In this paper, we demonstrate the cytotoxic activity of bispecific DARPin constructs against the HER2-addicted cell line BT474, a widely used model system for testing anti-HER2 activity in vitro. The bispecific DARPins not only induce a cytostatic effect like trastuzumab, but also act as specific cytotoxic agents. This cytotoxic effect does not rely on any conjugated toxin, but is intrinsic to the binding mechanism.

The results were confirmed on a broad panel of breast tumor cell lines and tumor models developed by R.T. and colleagues (R.T., M.S., C.J., D.C. Schaefer, G. Nagy-Davidescu, M. Göranson, A.H., and A.P., unpublished data), who proceeded to characterize in great detail the influence of these constructs on various aspects of downstream signaling, such as phosphorylation pattern, downstream kinase activity and apoptotic markers. They showed that the most potent of the bispecific DARPins cause a persistent inhibition of both the phosphatidyl-inositol-3-kinase (PI3K-AKT/PKB) and the RAS-RAF-MAPK pathway, leading to a strong apoptotic response.

Based on the X-ray structures of three DARPins in complex with the cognate HER2-ECD subdomain we have determined here, we propose a model of how such a complete shutdown of HER2-dependent signaling is achieved.

RESULTS

Epitope Mapping of HER2-Binding DARPins

DARPins that had been selected by phage display (Steiner et al., 2008) or ribosome display (Zahnd et al., 2007) to target the full-length ectodomain of HER2 without showing any cross-specificity against other EGFR-family members were characterized to determine which of the four HER2 subdomains forms the epitope. Since DARPins typically recognize conformational epitopes, we expressed subdomains alone and in combination in insect cells using a baculovirus system (Supplemental Experimental Procedures available online). To minimize glycosylation for subsequent crystallization, we replaced the Asn residues in predicted N-linked glycosylation sites by Asp. ELISAs on these proteins showed that the epitopes recognized by DARPins 9_26 and 9_29 are located on HER2-I, while DARPin G3 bound to HER2-IV (Figure S1A). Competition for binding to HER2-overexpressing cells measured by flow cytometry revealed that DARPins 9_26 and 9_29 compete for the same epitope (Figure S1B). DARPin G3, which binds to HER2 subdomain IV, did not compete with trastuzumab but competed with a different HER2-specific DARPin, H_14, which in turn competed with trastuzumab.

Construction of Bispecific Binders Targeting Different Epitopes

Various bivalent and bispecific constructs were generated by genetically fusing two DARPins by $(G_4S)_n$ linkers of different lengths. To target two nonoverlapping epitopes with a single molecule, DARPins 9_29 or 9_26 were connected to DARPin G3 by a 20-amino-acid linker, with either an ECD-I binder at the N-terminal end and the ECD-IV binder at the C terminus or in opposite orientation. The four different bispecific binders [e.g., 9_26-$(G_4S)_4$-G3, abbreviated "6_20_G" for the two DARPins and the linker length of 20 amino acids] were tested regarding their binding to HER2-overexpressing cells. G3 with a dissociation constant (K_D) of 90 pM (Zahnd et al., 2007) has the highest affinity of the three HER2 binders used in this study, compared to a K_D of 1 nM for 9_26 and 1 nM for 9_29 (Steiner et al., 2008). Kinetic experiments on cells in the presence of a competing DARPin (to prevent rebinding) revealed that the off-rates of the bispecific binders were ten times lower than the off-rates of monovalent G3 (Figure 1A; Table S1). The slower off-rate and lower K_D of the bispecific constructs, compared to their monovalent building blocks, can be attributed to an avidity effect and indicates bispecific binding to HER2 on the cell.

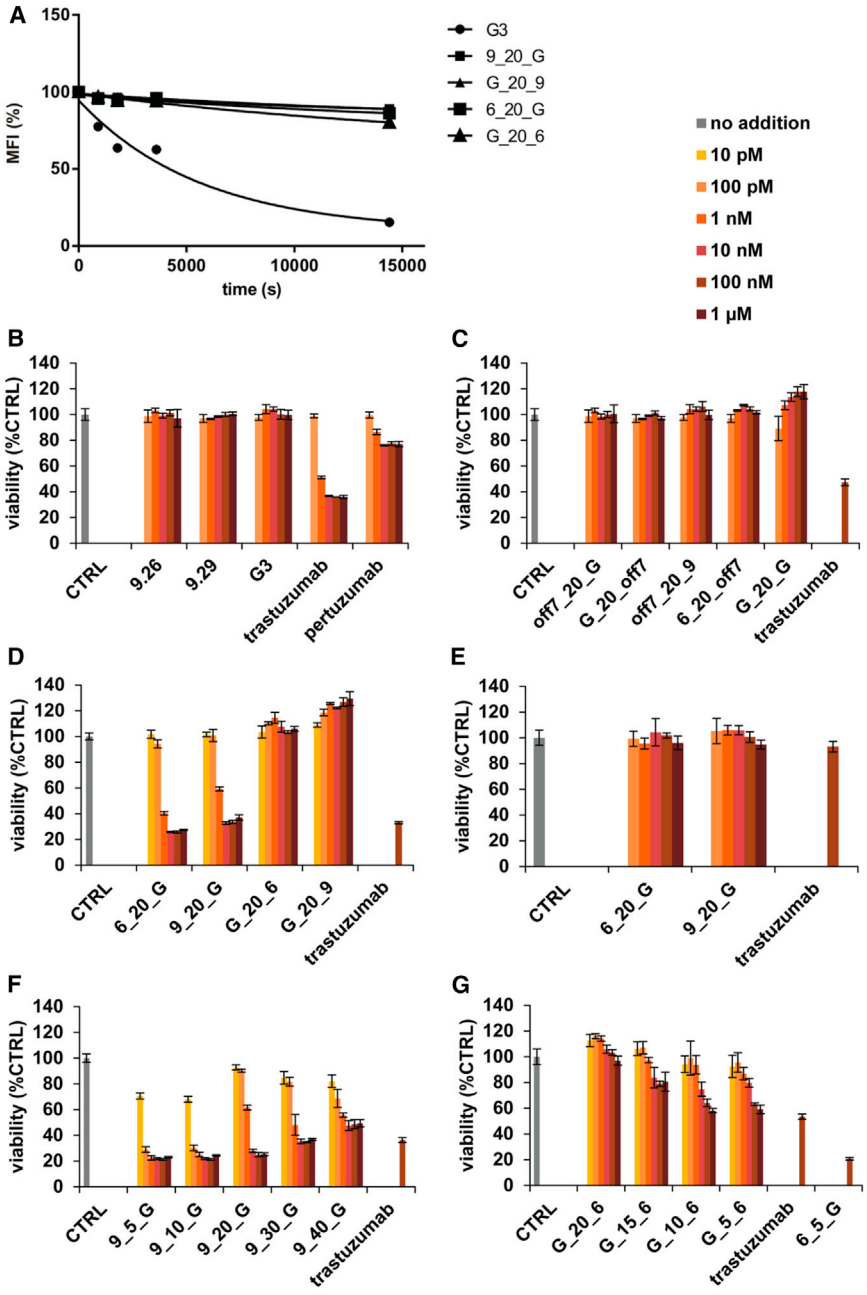

Figure 1. Biological Activity of DARPin Constructs

(A) Dissociation of monovalent and bispecific DARPins from the surface of BT474 cells. Median fluorescence intensities (MFI) of fluorescently labeled DARPins bound to the BT474 cell surface are plotted as a function of dissociation time. See Table S1 for fitted off-rates, Figure S1A for ELISA epitope mapping, and Figure S1B for binding competition on intact cells.

(B–G) Inhibition of cell proliferation was determined by XTT assays with HER2-addicted BT474 cells. Cells grew for 72 hr in the presence of different concentrations of DARPins. Bispecific DARPins 6_20_G and 9_20_G decreased the cell viability, whereas the reversely oriented constructs G_20_6 and G_20_9 did not. Cells that grew in the presence of 100 nM trastuzumab and cells growing without treatment served as control (CTRL). Error bars indicate SD. (B) Biological effects of monovalent DARPins. (C) Bispecific DARPins containing a nonbinding DARPin are shown. Off7 is a control DARPin recognizing maltose binding protein. G_20_G is homobivalent and contains twice the DARPin G3. (D) Biological effects of bispecific anti-HER2-DARPins on HER2-addicted BT474 cells and (E) on non-overexpressing MCF7 cells. (F) Effect of linker length on biological activity of bispecific DARPins in 9_x_G orientation or (G) in G_x_9 orientation.

Effects of Mono- and Bivalent Constructs on Cell Proliferation and Cell Death

We tested the influence of the different DARPin constructs on cell proliferation and cell survival in XTT assays, using BT474 cells as an example of a HER2-addicted cell line. MCF7-cells, which express HER2 at much lower levels than BT474 cells, were used as a control. Calibration experiments showed that a signal decrease by 60%, compared to untreated cells, corresponded to lack of cell proliferation over the 4 days of cell growth before the XTT assay; a larger decrease indicated cell death.

None of the monovalent DARPins characterized in this study affected the number of viable cells measured by the XTT assay (Figure 1B). Mixtures of two different DARPins proved to be equally inert, as did control constructs in which one of the two DARPins in the bispecific molecule had been replaced by a non-HER2-binding DARPin (DARPin off7, targeting maltose-binding protein; Binz et al., 2004) (Figure 1C). A monospecific bivalent DARPin, G_20_G, even stimulated cell proliferation (Figure 1C).

Bispecific constructs composed of a subdomain I binder at the N terminus and the subdomain IV binder at the C terminus (6_20_G or 9_20_G) showed a concentration-dependent decrease of cell viability by up to 75%, while treatment with trastuzumab decreased viability by ~50% (Figure 1D). The constructs with reverse orientation (G_20_9) either lacked any effect on cell growth (G_20_6) or even slightly promoted cell growth. Similar to trastuzumab, bispecific constructs did not affect the cell proliferation of MCF7 cells (Figure 1E), suggesting the restriction of the observed effects to HER2-addicted cells. Comparison of constructs with 5, 10, 20, 30 and 40 amino acid linkers showed that for 9_x_G constructs, specific activity and potency decreases with increasing linker length. The most potent constructs proved to be 6_5_G and 9_5_G, with (G_4S)-linkers of only five amino acids. They decreased the cell viability in XTT-assays after 4 days of growth by more than 80%, as compared to untreated cells, and showed a half-maximal effect already at a concentration of less than 100 pM compared to ca. 1 nM for 6_20_G and 9_20_G. Conversely, increasing the linker

Table 1. Statistics for Data Collection and Refinement

Complex	Statistics
HER2_I/9_29	
Data collection	
Space group	oP: $P2_12_12_1$
Cell dimensions, Å	a = 46.6, b = 80.5, c = 115.1
	$\alpha = \beta = \gamma = 90^\circ$
AU content	1 complex
VM, $Å^3$/Da	2.63
Resolution limits, Å	50 – 2.55
Observed reflections	total 53,167; unique 14,553; possible 14,772
Completeness, %	98.7 (99.4)*
R-merge	7.1 (40.7)*
I/σ	17.83 (4.01)*
Refinement	
Resolution range, Å	50-2.55
Final R-cryst, R-free, %	20.22, 25.39
Number of residues	331
Number of solvent molecules	31
Number of atoms	2559
Mean B-factor, $Å^2$	32.99
rmsd (bonds), Å	0.008
rmsd (angles), °	1.293
Ramachandran analysis, %	97.2/2.8/0
HER2_I/9_26	
Data collection	
Space group	mC: C2
Cell dimensions, Å	a = 138.5, b = 60.7, c = 107.2
	$\alpha = 90^\circ$, $\beta = 118.9^\circ$, $\gamma = 90^\circ$
AU content	2 complexes
VM, $Å^3$/Da	2.40
Resolution limits, Å	50 – 3.2
Observed reflections	Total 37,684, unique 12,785, possible 13,151
Completeness, %	97.2 (98.3)[a]
R-merge	7.1 (20.8)[a]
I/σ	14.37 (5.94)[a]
Refinement	
Resolution range, Å	50-3.2
Final R-cryst, R-free, %	31.31, 33.94
Number of residues	547
Number of solvent molecules	0
Number of atoms	3517
Mean B-factor, $Å^2$	48.66
rmsd (bonds), Å	0.004
rmsd (angles), °	0.766
Ramachandran analysis, %	88.7/9.6/1.7
HER2_IV/G3	
Data collection	
Space group	hR: R32
Cell dimensions, Å	a = 195, b = 195, c = 112
	$\alpha = 90^\circ$, $\beta = 90^\circ$, $\gamma = 120^\circ$
AU content	2 complexes
VM, $Å^3$/Da	1.95
Resolution limits, Å	50 – 2.65
Observed reflections	total 120,455; unique 23,767; possible 23,791
Completeness, %	99.9 (99.9)[a]
R-merge	4.1 (51.1)[a]
I/σ	26.42 (3.54)[a]
Refinement	
Resolution range, Å	50-2.65
Final R-cryst, R-free, %	21.32, 24.59
Number of residues	385
Number of solvent molecules	0
Number of atoms	2,808
Mean B-factor, $Å^2$	47.60
rmsd (bonds), Å	0.009
rmsd (angles), °	1.204
Ramachandran analysis, %	94.7/4.5/0.8

[a]Values in parentheses refer to the highest-resolution shell.

length to forty amino acids, as in 6_40_G and 9_40_G, decreased the biological activity (growth reduction of only 40%) (Figure 1F). The constructs with inverse orientation, G_x_6 and G_x_9, inactive or even stimulatory at a linker length of 20 amino acids, gained anti-proliferative activity at short linker lengths, but the best construct was found to be only as active as trastuzumab (Figure 1G).

Neither the single DARPins nor the bispecific constructs affected internalization or degradation of HER2, as determined by flow cytometry (R.T., M.S., C.J., D.C. Schaefer, G. Nagy-Davidescu, M. Göranson, A.H., and A.P., unpublished data).

X-Ray Crystal Structures of Complexes HER2_I:9_29, HER2_I:9_26, and HER2_IV:G3

The structures of the complexes of HER2_I with DARPin 9_29 and with 9_26 were determined at 2.55 Å and 3.2 Å resolution, respectively, the structure of HER2_IV in complex with G3 at 2.65 Å resolution. A summary of data collection statistics and refinement results is listed in Table 1. Unliganded 9_26 was solved to 2.9 Å (unpublished data), unliganded G3 (Protein Data Bank [PDB] ID 2JAB) (Zahnd et al., 2007) to 1.7 Å. G3 and unliganded 9_26 contain the original DARPin C-cap, which by NMR had been shown, to some percentage, to show some transient unfolding in solution (Wetzel et al., 2010). For crystallization in complex with HER2_I, this C-cap was replaced by an optimized C-cap (Mut5) (Interlandi et al., 2008) in DARPins 9_29 and 9_26, which does not give any sign of transient unfolding.

The asymmetric unit of HER2_I:9_29 contains one heterodimeric complex with seven intermolecular hydrogen bonds (Table S2) and a buried surface area of 784 $Å^2$ (Figures 2A–2C). In the

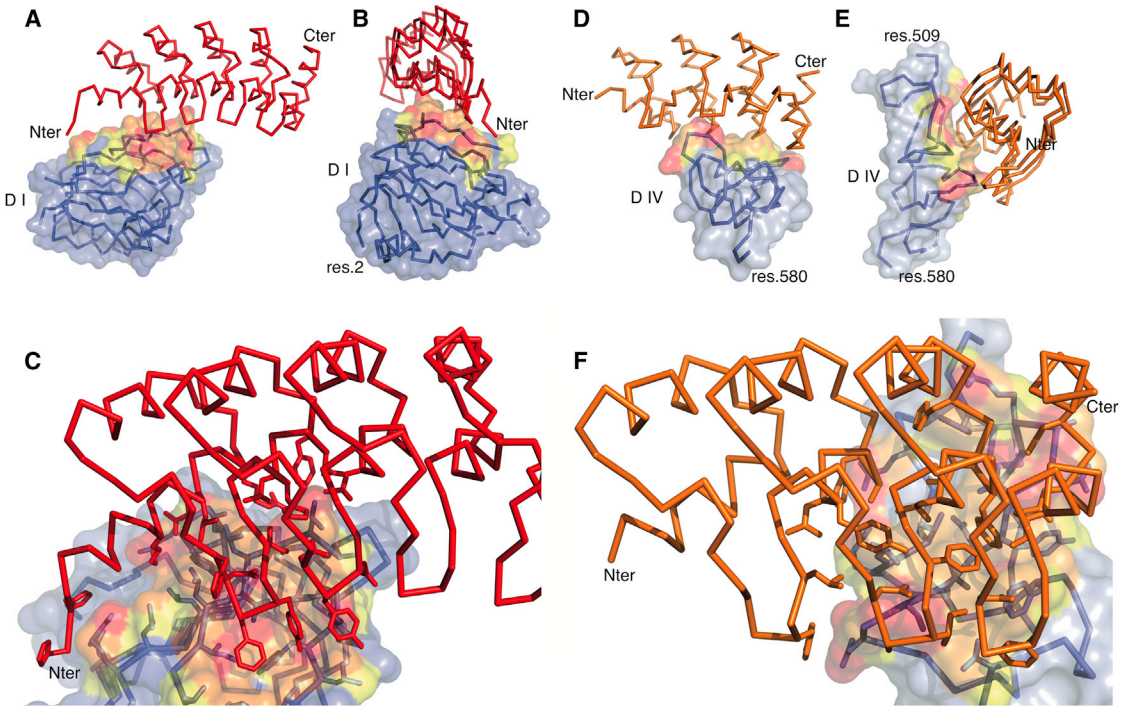

Figure 2. Structures of DARPin:HER2 Complexes

DARPins 9.29 (red) and G3 (orange) in complex with HER2 subdomain I and IV, respectively (blue). HER2 residues having at least one nonhydrogen atom within 5.0 Å of a nonhydrogen atom of the DARPin (i.e., epitope residues) are shown in yellow, those with atoms within 5.0 Å of the DARPin (solvent excluding contacts) in orange, and those with atoms within 3.6 Å (Van-der-Waals contacts) in red.

(A–C) DARPin 9_29 in complex with HER2_I.

(D–F) DARPin G3 in complex with HER2_IV.

(C and F) Close-up of epitope and paratope: side chains of residues having at least one nonhydrogen atom within 5.0 Å of a nonhydrogen atom of HER2 (paratope residues) are shown in stick representation.

See Figure S2 for superpositions of the HER2 subdomains on the full-length HER2_ECD and Table S4 for rmsd values.

asymmetric unit of HER2_I:9_26, two heterodimers are present. Due to the limiting quality of the HER2_I:9_26 data set, the slight differences that are visible between the two complexes of the asymmetric unit leave some minor uncertainty about the exact geometry of the binding of DARPin 9_26. Most of our analyses are therefore concentrated on the HER2_I:9_29 complex. However, despite the lower resolution of the HER2_I:9_26 structure compared to the HER2_I:9_29 structure, two crucial conclusions can be drawn from the presented structure: the buried surface area, and more importantly the orientation, of 9_26 are very similar to the mode of binding of the better resolved 9_29 to HER2_I. The asymmetric unit of the HER2_IV:G3 structure contains two heterodimeric complexes with 7 and 5 intermolecular hydrogen bonds between DARPin G3 and HER2_IV (Table S3), respectively, and a buried surface area of 818 $Å^2$ (complexes A/D, Figures 2D–2F) or 759 $Å^2$ (complex B/C).

The conformation of HER2_I and HER2_IV is essentially the same as that of the respective subdomain in structures of the whole extracellular domain of HER2 (Cho et al., 2003; Garrett et al., 2003; Franklin et al., 2004; Bostrom et al., 2009; Fisher et al., 2010), with root-mean-square deviation (rmsd) values for the Cα-backbone around 0.49 to 0.81 Å for HER2_I and 0.24 to 0.68 for HER2_IV (Table S4; Figures S2A and S2B), underlining the rigidity of the HER2 domains.

A comparison of the epitopes recognized by various HER2 binders in the Protein Data Bank (Figure 3) shows that the regions recognized by the three DARPins do not overlap with epitopes recognized by any of the other binders: scFv A21 binding to domain I (Zhou et al., 2011), therapeutic antibody pertuzumab recognizing subdomain II (Franklin et al., 2004), Z-domain-derived affibody zHER2 (Eigenbrot et al., 2010) recognizing the same epitope on domain III as Fab37 (Fisher et al., 2010), and trastuzumab (Cho et al., 2003) and its HER2/VEGF dual specific variant bH1 (Bostrom et al., 2009) binding to subdomain IV.

DARPins 9_29 and 9_26 bind to the same epitope on HER2_I, involving residues from the N-cap and the first two internal repeats (Figure 4). The third repeat and the C-cap make no contacts. The DARPin contacts two adjacent strands of HER2_I at the edge of this domain, including further interactions down the side perpendicular to the β helix axis of domain I, which is a member of the L-domain family. The high-affinity binding of DARPin 9_29 to HER2_I is governed by six hydrogen bonds, π-stacking, and extended hydrophobic interactions described in detail in Supplemental Experimental Procedures and Table S2. Epitope and paratope residues are highlighted in the sequence alignments shown in Figure S3. Comparison of the sequence differences between the two DARPins to this contact map shows that 14 out of 19 contact residues are conserved.

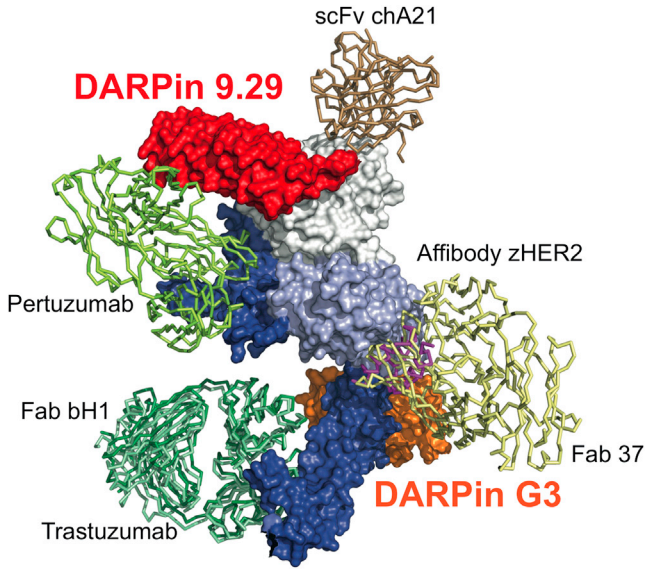

Figure 3. Superposition of HER2 Complexes on the Full-Length HER2 ECD

DARPin 9_29 (PDB ID 4HRL, red) is binding to subdomain I, DARPin G3 (PDB ID 4HRN, orange) to subdomain IV. In addition, Fab fragments of the therapeutic antibody trastuzumab (Herceptin, PDB ID 1N8Z, pale green), its derived HER2/VEGF dual specific variant bH1 (PDB ID 3BE1, forest green), and pertuzumab (Perjeta, PDB ID 1S78, lime) are shown, as well as Fab 37 (PDB ID 3N85, pale yellow), scFv chA21 (PDB ID 3H3B, sand color), and Z-domain affibody zHER2 (PDB ID 3MZW).

Construct HER2-IV spans residues 509–604 of the HER2-ECD, omitting the last two disulfide bonds. Residues 581–604 are disordered in the structure. DARPin G3 binds to an epitope on the N-terminal half of subdomain IV (residues 513–564). The structure of G3 in the complex is well maintained compared to its uncomplexed structure (rmsd 0.65 or 0.55 Å; Figure S2C), demonstrating that the DARPin:HER2 complexes can, in a first approximation, be considered as rigid-body interactions. The paratope comprises both internal repeats and the C-cap of the DARPin (Figure 2; Figure S3). The long axis of the DARPin is at nearly a right angle to the long axis of HER2_IV, the DARPin β-turns facing toward the membrane. The DARPin wraps around the rod shaped Cys-rich domain IV, its slight curvature is fitting the target shape very well, explaining the high affinity of 90 pM. It contacts two protrusions, formed by the loop spanned by Cys 523 and 539 and the adjacent pair of interlocked disulfide bond. Two of the four mutations introduced during affinity maturation are directly involved in binding interaction. Of the 14 randomized residues, 9 are involved in specific contacts, as are several framework residues. Six hydrogen bonds and extended hydrophobic interactions, altogether contributed by 13 residues (Supplemental Experimental Procedures), are responsible for the picomolar affinity of G3. The atomic interactions are summarized in Table S3. Thus, although G3 possesses only two internal repeats, the perfectly matching hydrophobic and hydrogen bonding interactions, contributed by adapted curvature as a result of directed evolution (Zahnd et al., 2007), account for its high affinity.

Molecular Modeling of Full HER2 and DARPin-Inhibited States

Since the HER2 domains are very rigid and their structure did not change between the DARPin complexes and the whole ECD, we could easily place the DARPins on the full HER2_ECD (residues 1–620). We also built models of putative HER2_ECD homo- and heterodimers (see Supplemental Experimental Procedures for a detailed description of the modeling procedure), taking into account all available ErbB-family structures to make the models as realistic as possible. The DARPins bound to HER2_I and HER2_IV could be added to the HER2 monomer and dimer models without any clashes (Figures 5A–5D).

To build a model of the whole receptor, the HER2-ECD model was combined with the NMR structures of transmembrane helices (PDB ID 2JWA; Bocharov et al., 2008) and the X-ray structures of the kinase domains (PDB ID 3PP0 for the active kinase dimer [Aertgeerts et al., 2011] and 3RCD for the inactive kinase [Ishikawa et al., 2011]), taking the electron-microscopy-based models of Mi et al. (2011) as a guide. Seven residues between the last disulfide bridge of ECD domain IV and the start of the transmembrane helix and 30 residues between TM domain and kinase were treated as flexible to connect the domains.

The resulting models assume that initially both monomer and dimer stand upright on the membrane and that the HER2-ECD is as rigid as suggested previously (Cho et al., 2003; Dawson et al., 2007).

The distance between the C-term of the domain I-binding DARPin and the N-term of the domain-IV-binding DARPin is 130 Å on the same HER2 molecule (Figure 5A). For intramolecular binding to a HER2_ECD monomer in this orientation, 9_x_G, the linker would have to be even longer, as it needs to wrap around the monomer. However, the most active of our constructs has a linker length of a mere five amino acids, spanning no more than 17 Å, which thus excludes intramolecular binding (Figure S4).

To connect two DARPins on the same side of the HER2 homodimer (Figures 5C and 5D), the linker would have to span at least 80 Å for the 9_x_G construct, and to connect DARPins on two independent monomers, the linker would have to span at least the difference in height above the membrane of the two termini, more than 50 Å. It follows that with the most active of our constructs, with a 17 Å linker, linking two HER2 molecules in either of these upright conformation is not possible.

Since the observed biological activity and increased binding avidity of the short-linkered constructs prove that the bispecific constructs do bind bivalently on cells, it follows that the HER2 molecules must arrange to accommodate this. For bivalent binding of 9_5_G to occur, the 9_29 epitope of HER2_I has to move closer to the membrane, and this requires either a major conformational change within the HER2_ECD (which is unlikely, as explained below), or a major change in the orientation of the whole HER2-ECD relative to the membrane, moving essentially as a rigid body.

Comparison of extracellular domain conformations in various different ErbB family crystal structures indicates that there are very few possibilities for major conformational changes within the HER2_ECD. The connection between subdomains I and II and between III and IV is quite rigid: the side chain of conserved Trp 183 of subdomain II inserting into the core of subdomain I and the side chain of Trp 499 of subdomain IV inserting into

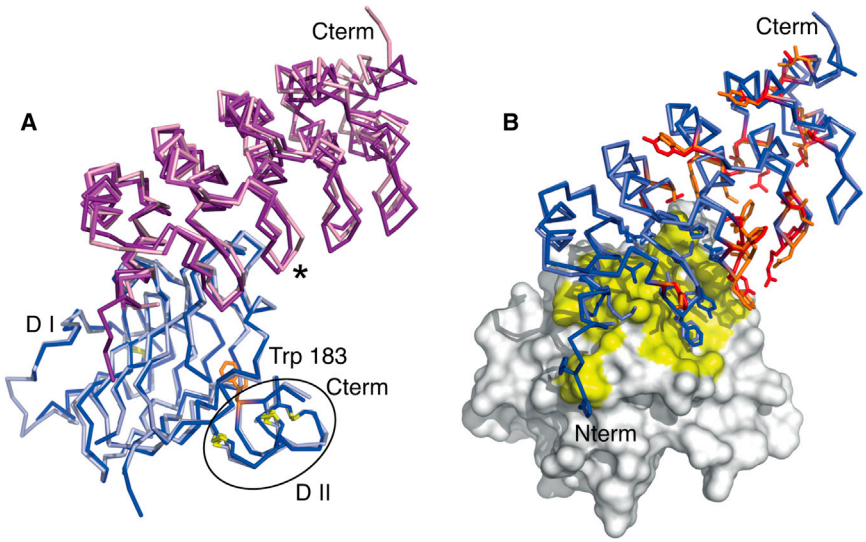

Figure 4. Comparison of DARPin 9_26 and 9_29 Complexes with HER2-I

(A) Superposition of the HER2_I:DARPin 9_29 complex structure (HER2_I: dark blue, 9_29: purple) onto the HER2_I:DARPin 9_26 complex structure (HER2_I: pale blue, 9_26: magenta). The two structures were superimposed by a least-squares fit of the Cα positions of HER2_I residues 21–96 and 116–152 (rmsd 0.53 Å). Unliganded DARPin 9_26 (2.9 Å resolution, pale pink) was superimposed on the DARPin in the HER2_I:9:26 complex. A one-residue deletion in the second loop of DARPin 9_29 is indicated by (*).

(B) Sequence differences between DARPins 9_29 (dark blue) and 9_26 (pale blue). DARPin 9_26 was superimposed on DARPin 9_29 in the HER2_I:DARPin 9_29 complex structure. Side chains of conserved paratope residues (blue) and divergent DARPin residues (9_29, red; 9_26, orange) are shown in stick representations.

See Figure S3 for a sequence alignment.

the core of domain III severely limit the flexibility of these interfaces. Major conformational changes within ErbB receptor extracellular domains appear to be limited to a rigid-body movement of the domain I–II pair relative to the domain III–IV pair around a pivot between domains II and III (Cho et al., 2003). HER1, HER3, and HER4 occur in two conformational states. In the presence of an activating ligand, their extracellular domain assumes an "open" conformation, similar to the default conformation of the HER2_ECD (Ogiso et al., 2002; Liu et al., 2012), while their default conformation in the absence of a ligand and/or dimerization partner is a "tethered" conformation (Cho and Leahy, 2002; Ferguson et al., 2003; Bouyain et al., 2005), which has so far not been observed for HER2. The HER2_ECD constitutively assumes an "open" conformation (Garrett et al., 2003).

However, a rigid HER2_ECD could easily tilt relative to the membrane (Figures 6D and 6G). This would require flexibility in the short peptide segment between the last disulfide-bridged cysteine of the extracellular domain and the start of the transmembrane helix. Indeed, these residues are disordered in reported structures of the HER2 extracellular domain and in NMR structures of the transmembrane helix. Based on single-molecule Förster resonance energy transfer analysis and fluorescence lifetime imaging microscopy, this region in EGFR has been proposed to be sufficiently flexible to allow the EGFR_ECD to equilibrate between an upright position and one lying flat on the membrane (Webb et al., 2008). Thus, tilting the ECD in such a way that the dimerization loop points toward the membrane (Figures 6D and 6G) would lower the C terminus of 9_29 (or 9_26, respectively) and raise the N terminus of G3 in such a way that the two can be connected by a short linker.

Alternatively, a hypothetical pseudo-tethered conformation of HER2, for which, however, there is currently no direct evidence, would bring the 9_29 epitope into an ideal position relative to the G3 epitope of a second HER2 monomer for intermolecular crosslinking with short-linkered constructs (Figures 6C and 6F), while intramolecular crosslinking within a tethered monomer would still require a 70 Å (G_x_9) to 80 Å (9_x_G) linker. Such a conformation would not interfere with DARPin binding, but would prevent the formation of back-to-back HER2 homo- and heterodimers.

The most important deduction from these models is that, by linking domain I of one HER2 molecule to domain IV of another by a short linker, the transmembrane domains of the two HER2 are forced apart. This conclusion is independent of the pivot point utilized and independent of the exact geometry of the HER2:DARPin:HER2 complex. The consequence of the DARPin-induced movement of domains I and IV of two different HER2 molecules is that it prevents the assembly of active kinase dimers.

DISCUSSION

The results presented in this paper and the associated models of the induced inhibited states of HER2 allow us to propose a mechanism of the induction of cytotoxicity within the framework of activation and inhibition of the ErbB receptor family. We present the X-ray structures of three DARPin:target complexes, with DARPins 9_29 and 9_26 binding to the same epitope on subdomain I of HER2, and DARPin G3 recognizing subdomain IV. The structures of the DARPins in complex with the cognate receptor domain can be superimposed on the structure of the full-length HER2 extracellular domain without any evidence for conformational changes in the individual domains beyond some very small local flexibility, already apparent from the comparison of the various structures of HER2_ECD in the Protein Data Bank. Thus, the superposition of the DARPins on the whole HER2 ECD is unambiguous.

Monomeric DARPins Do Not Interfere with HER2 Signaling

All tested monovalent DARPins that were used for the construction of the bispecific binders, individually or as a mixture, have no effect on the cell survival and proliferation of cultured BT474 cells, indicating that the monovalent DARPins do not interfere with HER2 signaling in this HER2-addicted cell line. Models of the putative HER2 "back-to-back" homodimer (Figure 6B) or of canonical heterodimers with EGFR or HER3 (not shown), which are generally thought to represent the active state of HER2, indicate indeed that the binding of unlinked

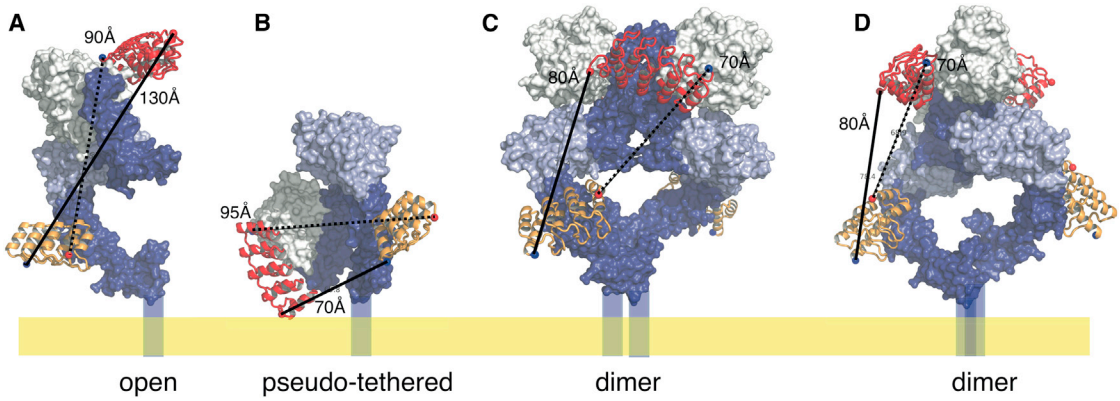

Figure 5. Distances between DARPin N and C Termini

(A) For bivalent binding to a HER2 monomer, the linker in a 9_x_G construct would need to span a distance of 130 Å (solid line), plus enough slack added to wrap around HER2. In a G_x_9 constructs, the two termini would need to span 90 Å (broken line).

(B) To bind to a HER2 monomer in a pseudo-tethered conformation, 70 Å (9_x_G construct) or 95 Å (G_x_9 construct) would have to be bridged.

(C and D) To connect two DARPins bound to the same side of a HER2 dimer, 80 Å would have to be bridged by a 9_x_G construct, 70 Å by a G_x_9 construct. (C) and (D) show the same dimer, rotated by 90° around the y axis.

Linker lengths in the various bispecific DARPins vary from 16.5 Å (9_5_G) to 132 Å (9_40_G), assuming a fully extended conformation (Figure S4).

(i.e., monovalent) DARPins should not interfere with homo- or heterodimerization, consistent with the observation that the monovalent DARPins are not biologically active. Since the monovalent DARPins cover both sides of the dimer, they should interfere with the lateral association of receptor dimers to produce tetramers or higher oligomers formed by stacking the planes defined by domains I, II, and III, as recently proposed (Zhang et al., 2012). However, since the unlinked DARPins do not interfere with HER2 activity, higher oligomers associating in this specific manner cannot be required for the activity of HER2 measured in our assays.

Activity Depends on Linker Length

When connected by short flexible linkers, the two DARPins 9_29 and G3 acquire biological activity. While monospecific bivalent constructs, in particular G_20_G, activate HER2 signaling and have a proproliferative effect on BT474 cells, presumably by stabilizing HER2-HER2 homodimers, the bispecific bivalent constructs described here inhibit HER2 signaling and decrease cell viability, without affecting the number of receptors displayed on the cell surface (R.T., M.S., C.J., D.C. Schaefer, G. Nagy-Davidescu, M. Göranson, A.H., and A.P., unpublished data). Their activity is dependent on linker length and on domain orientation. Constructs with shorter linkers show higher activity than constructs with longer linkers, and constructs with N-terminal DARPin 9_29 and C-terminal DARPin G3 (9_x_G) show significantly higher activity than G_x_9, the opposite orientation, of the same linker length. While for the G_x_9 orientation the inhibitory activity already disappears with a linker length of 20 amino acids, in the 9_x_G orientation, even the construct equipped with a 40-amino-acid linker shows some activity.

Constructs in which one of the DARPins has been replaced by the nonbinding DARPin off7 are biologically inactive, demonstrating the need for bivalency. Therefore, we have to conclude that the biological activity of the bispecific constructs is indeed due to crosslinking of HER2 molecules and not to simple direct steric hindrance of HER2 homo- or heterodimerization by the DARPins.

The Linker Length Is Too Short for Both DARPins to Bind to the Same HER2 Monomer or Dimer

The linkers of the shortest and most potent of the bispecific constructs tested, 9_5_G, 9_10_G, and 9_20_G, are too short to connect the C terminus of 9_29 to the N terminus of G3 bound to the same HER2 molecule, in either the open conformation seen in all crystal structures of the HER2 ectodomain (Cho et al., 2003; Franklin et al., 2004; Bostrom et al., 2009; Eigenbrot et al., 2010; Fisher et al., 2010) or in a hypothetical pseudo-tethered conformation modeled in analogy to the tethered conformations of other members of the ErbB family (Cho and Leahy, 2002; Ferguson et al., 2003; Bouyain et al., 2005; Li et al., 2005; Hollmén et al., 2012; Liu et al., 2012; Ramamurthy et al., 2012). The linkers are also too short to connect DARPins bound to the two HER2 monomers in a putative back-to-back HER2 homodimer. The observed bivalent binding, therefore, can only be explained by crosslinking of two independent HER2 monomers, at least one of which has to bend down (see below).

Orientation of HER2 on the Cell Surface

On the surface of intact cells, the transmembrane domain of the receptor is constrained to the plane of the membrane, restricting translational and rotational freedom of the receptors. Conventionally, receptors of the ErbB family are depicted as standing upright on the cell surface, with their main axis about perpendicular to the plane of the membrane. However, it has been proposed that a small percentage of EGFR, providing high-affinity EGF sites, can lie flat on the surface (Webb et al., 2008), underlining the flexibility of the few residues between the receptor ectodomain and the TM helices to allow this. Therefore, a tilting of the whole ectodomain of HER2 with a pivot close to the membrane has some precedent.

Nonetheless, a completely flat orientation of HER2 dimers is inconsistent with binding of DARPins, as in the bound state

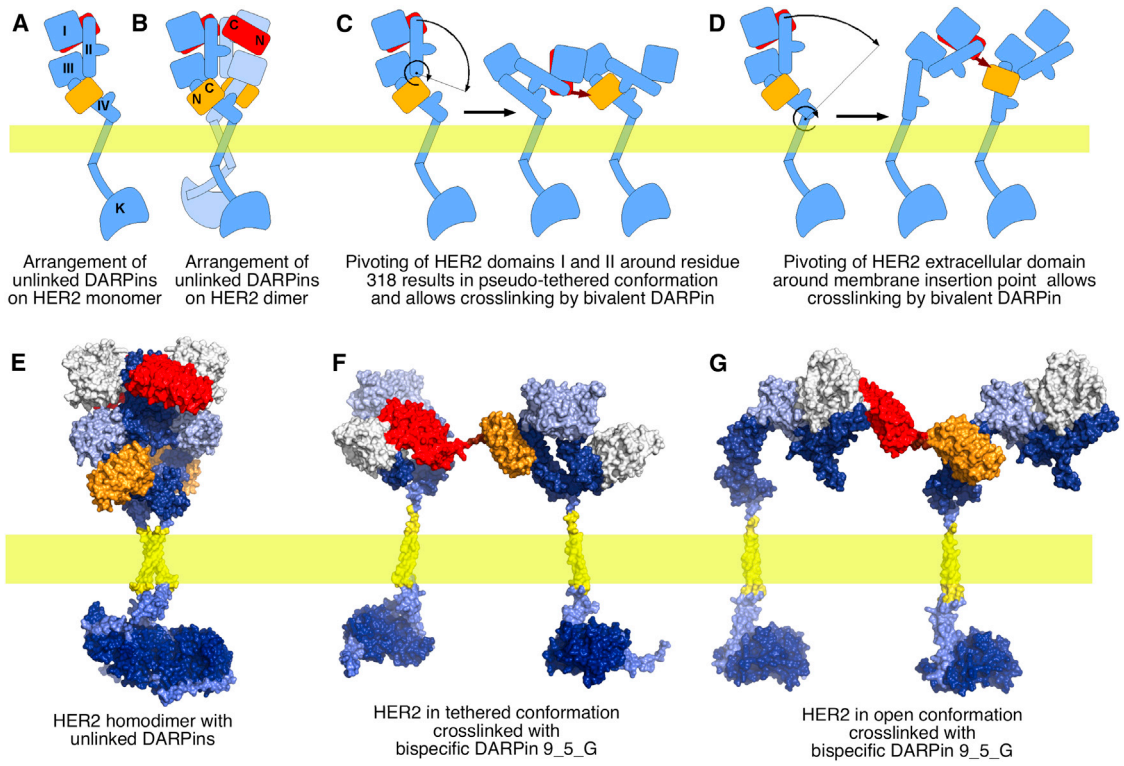

Figure 6. Putative Models of Full-Length HER2 Complexed by Monovalent or Bispecific DARPins

A model of the complete structure of HER2 in complex with the two DARPins 9_29 and G3 was generated as described in Supplemental Experimental Procedures.

(A, B, and E) Unlinked DARPins 9_29 (red) and G3 (orange) are modeled to bind to putative HER2 homo- and heterodimers and are predicted to not interfere with receptor dimerization.

(C, D, F, and G) Bispecific DARPins with short linkers can only crosslink two HER2 molecules if domain I is brought closer to the membrane through binding of the DARPin.

(D and G) Domain I is brought closer to the membrane by pivoting the rigid extracellular domain (ECD) around a point in a short flexible peptide between the last disulfide bridge in domain IV and the start of the transmembrane helix. This would allow bispecific DARPin 9_5_G to bind two HER2 molecules with ECDs in the open conformation found in all structures of the HER2_ECD.

(C and F) Alternatively, a rotation around the pivot point utilized in the transition between open and tethered conformation (Arg 317) of other ErbB members would yield a pseudo-tethered conformation that brings domain I closer to the membrane and allows bispecific DARPin 9_5_G to crosslink two HER2 molecules with ECDs in a (putative) tethered conformation.

Both models (B/F and C/G) enforce a large distance between the kinase domains, and both prevent further dimerization by the strong tilt of dimerization interfaces and/or by making the dimerization loop inaccessible. Both models would also be compatible with daisy-chaining, forming higher-order oligomers.

they would prevent a flat orientation, since DARPin epitopes would be located between receptor and membrane. Also, since the majority of receptors is standing upright in EGFR (Webb et al., 2008), there must be a dynamic equilibrium, and any bound DARPin will shift this equilibrium away from any flat orientation. Considering the data on EGFR, it follows for HER2 that a tilted orientation of HER2 molecules in the DARPin-linked state is possible, but not a completely flat one. This flat orientation, which we can exclude, would be the only one in which the TM helices would be able to come close enough for the kinases to form an active dimer.

Conformational Flexibility of the HER2 Extracellular Domain

Our experiments show that even the shortest linker, spanning less than 17 Å in extended conformation, allows bivalent binding of the bispecific DARPins. Since such bivalent binding is not possible for the open, fully erect conformation of the extracellular domain, something has to bend. The interfaces between domain I and II and between domain III and IV are rigid. The side chain of Trp 183 in cysteine-rich domain II is buried in the core of domain I, and the side chain of Trp 499 of cysteine-rich domain IV is buried in the core of domain III, allowing only very limited flexibility. HER2_I_II and HER2_III_IV can therefore be regarded as structurally rigid units. Only two positions in the extracellular domain have the potential to act as a pivot for allowing large-scale conformational changes: either a hinge motion around the boundary residue between domain II and III (a Lys in EGFR, HER3, and HER4, corresponding to Arg 317 in HER2), which relates the open to the tethered conformation in other ErbB family members (Figures 6C and 6F), or more likely (regarding the probable constitutively open conformation of HER2_ECD) a tilting of the whole ECD relative to the membrane, relying on the flexibility of the residues

between the last cysteine of domain IV and the transmembrane helix (Figures 6D and 6G).

Interference with HER2 Dimerization and Activation

Either of the two discussed putative conformational changes captured by the bispecific DARPins leads to a situation where the back-to-back dimerization interface of HER2 is obstructed. In any pseudo-tethered conformation, this obstruction is intramolecular; in any of the conceivable tilted conformations, it is due to the enforced proximity of the dimerization interface to the membrane. Either model, and all reasonably conceivable geometric variations of the models, would result in bringing the C terminus of DARPin 9_29 closer to the N terminus of DARPin G3. As the transmembrane helices cannot be pulled out of the plane of the membrane, this forces the membrane insertion points and therefore the transmembrane and intracellular kinase domains apart, independent of the pivot point.

For maximal inhibition, formation of larger oligomers formed by daisy-chaining may be required, where every receptor monomer is bound to two bispecific DARPins and both DARPin epitopes on HER2 are occupied. For linker lengths exceeding 20 amino acids, alternative, intramolecular binding modes may start to compete with the intermolecular binding modes enforced by the short linker, explaining their overall lower biological activity.

Conclusions

The contrast between the biological inertness of the monovalent DARPins alone or in combination, the stimulation of HER2 signaling by monospecific bivalent DARPin construct G_20_G and, on the other hand, the potent inhibition of HER2 signaling by bispecific DARPin constructs connected by a minimal linker is intriguing. Trivial explanations for the inhibitory activity of the bispecific constructs, such as receptor downregulation or direct steric hindrance of receptor dimerization, could be excluded (R.T., M.S., C.J., D.C. Schaefer, G. Nagy-Davidescu, M. Göranson, A.H., and A.P., unpublished data), leaving a model where the steric constraints imposed by the membrane anchoring of the receptors play an important role in forcing apart the transmembrane helices of two HER2 monomers connected by the bispecific DARPin constructs.

The large fraction of the HER2 dimer surface covered by the biologically inert monovalent DARPins challenges models that postulate a need for lateral tightly packed HER2-oligomers for certain aspects of HER2 signaling in the cell line described here. The strong inhibitory effect of the bispecific DARPin constructs makes them an interesting starting point for future tumor targeting constructs directed against HER2-addicted cancer cells. A detailed analysis of their effects on different aspects of downstream signaling is presented in a separate publication (R.T., M.S., C.J., D.C. Schaefer, G. Nagy-Davidescu, M. Göranson, A.H., and A.P., unpublished data).

In summary, the engineering of binding molecules that bispecifically target HER2 at domains I and IV, connected by a linker not commensurate with intramolecular binding or binding to back-to-back complexes, has proven to be a very promising way to expand the arsenal of molecular targeting of cancer cells that are addicted to this receptor. In this context, DARPins might be particularly promising, as they can be easily engineered in a variety of molecular orientations and equipped for prolonged systemic circulation in order to extend their outstanding in vitro potency for in vivo studies (R.T., M.S., C.J., D.C. Schaefer, G. Nagy-Davidescu, M. Göranson, A.H., and A.P., unpublished data).

EXPERIMENTAL PROCEDURES

Cloning, Expression, and Purification of DARPins

All DARPins were purified essentially as described previously (Zahnd et al., 2010). Proteins were overexpressed in *E. coli* XL1-Blue and purified via their N-terminal $MRGSH_6$ tag with nickel-nitrilotriacetic acid superflow resin (QIAGEN). For cloning of bispecific constructs, the DARPin ORFs were digested with BamHI and HindIII (New England Biolabs) and ligated into compatible expression vectors pQiBi, coding for different flexible $(G_4S)_n$ linkers. This results in the connecting …AEILQKL$(G_4S)_n$RSDLGKKLL…, where the first underlined sequence is from the C-cap of the N-terminal DARPin, the second underlined sequence is from the N-cap of the C-terminal DARPin and n indicates the number of pentapeptides present in the flexible linker.

Cell Culture

BT-474 cells were obtained from the American Type Culture Collection (ATCC HTB-20). Cells were grown in complete RPMI 1640 medium (Sigma-Aldrich) supplemented with 10% (v/v) heat-inactivated FCS (PAA GmbH) and 100 U/ml penicillin/streptomycin (Sigma) in a humidified incubator with 5% CO_2.

Flow Cytometry

Per assay, 1×10^6 cells were incubated with the respective fluorescently labeled DARPins at the indicated concentrations in 100 µl PBS_BA (PBS, 0.2% NaN_3, 1% BSA). After incubation, cells were harvested by centrifugation (800 × *g*, 30 s, 4°C) and washed twice using 1 ml PBS_BA, each. Flow cytometry was performed on a Cyflow space system (Partec). Recorded events were gated for FSC/SSC of single viable cells. Fluorescence data were analyzed using the FlowJo software.

Dissociation experiments were performed as described in (Tamaskovic et al., 2012). In brief, aliquots of 1×10^6 cells were preincubated with DARPin-AlexaFluor488-conjugates at 100 nM in PBS_BA for 1 hr at room temperature. Cells were washed twice as described above and dissociation was allowed to proceed in the presence of unlabeled DARPin for the times indicated shaking at room temperature, followed by washes and flow cytometry measurements as described above.

Cell Viability Assays

BT474 cells were seeded at a density of 10,000 cells/cm^2 in 96-well-plates (Nunc). After 24 hr, DARPins (or trastuzumab as control) were added and cells were incubated for another 72 hr. Cells were then incubated with 50 µl/well 2,3-bis(2-methoxy-4-nitro-5-sulfophenyl)-2H-tetrazolium-5-carboxanilide (XTT; Roche) for 4 hr at 37°C. Absorbance was measured at 450 nm and expressed as percentage of the untreated controls.

Expression in Insect Cells

Recombinant HER2-ectodomains carrying an N-terminal melittin signal sequence and an N-terminal His_6 tag were expressed in *Spodoptera frugiperda* (Sf9) cells. Baculoviruses for infection of Sf9 cells were generated using the Multibac system as described (Fitzgerald et al., 2006). Sf9 cells were grown to a density of 4×10^6 cells/mL and coinfected with the respective virus at a MOI of 1. Then 72 hr post infection, cells were harvested by centrifugation (30 min, 5,000 *g*, 4°C) and the cleared medium was subjected to immobilized metal ion affinity chromatography (IMAC) purification with Ni-NTA Superflow (QIAGEN) purification resin.

X-Ray Crystallography

HER2_I and HER2_IV were expressed and purified as described above. After preincubation with DARPins 9_26_Mut5, 9_29_Mut5 or G3 at equimolar

concentrations, complexes were purified via size exclusion chromatography on a Superdex 200 HiLoad 16/60 column equilibrated with TBS150 (PBS, 150 mM NaCl). Eluted protein was concentrated to 14 (9_26/HER2_I), 8 (9_29/HER2_I), or 9 (G3/HER2_IV) mg/ml using Millipore Amicon Ultra 10K centrifugal concentrators. Crystals of the complexes formed in sitting drops mixed with two parts protein solution and one part mother liquor. The mother liquor contained 0.2 M NaCl, 0.1 M phosphate citrate (pH 4.2), and 20% PEG 8000 for 9_26/HER2_I; 0.2 M ammonium acetate (pH 5.6), 0.1 M sodium citrate, 30% (w/v) PEG 4000 for 9_29/HER2_I, or 0.05 M succinic acid and 29% ammonium sulfate (pH 4.0) for G3/HER2_IV, respectively. Crystals grew within 3 days (9_29/HER2_I), 3 weeks (9_26/HER2_I) or 4 weeks (G3/HER2_IV), respectively. They were then transferred to a cryoprotectant solution containing 20% glycerol. Data were collected using the PILATUS 2 M detector system on the PXIII beam line at the Swiss Light Source (Paul Scherrer Institute) and processed using the program XDS (Kabsch, 2010). The structures were solved by molecular replacement using PHASER MR (McCoy et al., 2007) from within the CCP4 package (CCP4, 1994). Model building was carried out by using the program COOT (Emsley et al., 2010). The structures were refined using PHENIX (Adams et al., 2010). Stereochemical properties were analyzed with MOLPROBITY (Davis et al., 2007) and structure figures were generated in PYMOL (http://pymol.org).

Statistical Analysis

Results from cell viability assays and ELISA experiments were expressed as means from triplicate measurements in bar graphs. Error bars indicate SD.

ACCESSION NUMBERS

The HER2_I/9_29, HER2_I/9_26, and HER2_IV/G3 structures have been deposited in the Protein Data Bank (http://www.pdb.org) under the codes 4HRL, 4HRM, and 4HRN, respectively.

SUPPLEMENTAL INFORMATION

Supplemental Information includes Supplemental Experimental Procedures, four figures, and four tables and can be found with this article online at http://dx.doi.org/10.1016/j.str.2013.08.020.

AUTHOR CONTRIBUTIONS

C.J., J.S., R.T., M.S., and A.P. designed research; C.J., J.S., and M.S. performed research; C.J., J.S., A.H., and A.P. analyzed data; and C.J., A.H., and A.P. wrote the paper.

ACKNOWLEDGMENTS

We thank Céline Stutz-Ducommun and Beat Blattmann for help in protein crystallization and the staff of beamline PXIII at the Swiss Light Source for support during data collection. This work was supported by the Swiss National Center of Competence in Research in Structural Biology, Schweizerischer Nationalfonds grant 3100A0-113720, and Krebsforschung Schweiz grant KFS-02448-08-2009. C.J., R.T., M.S., and A.P. have applied for a patent on findings related to this manuscript. A.P. is a co-founder and shareholder of Molecular Partners AG, which is commercializing the DARPin technology. J.S. is now an employee of Molecular Partners AG.

Received: May 29, 2013
Revised: August 25, 2013
Accepted: August 26, 2013
Published: October 3, 2013

REFERENCES

Adams, P.D., Afonine, P.V., Bunkóczi, G., Chen, V.B., Davis, I.W., Echols, N., Headd, J.J., Hung, L.W., Kapral, G.J., Grosse-Kunstleve, R.W., et al. (2010). PHENIX: a comprehensive Python-based system for macromolecular structure solution. Acta Crystallogr. D Biol. Crystallogr. *66*, 213–221.

Aertgeerts, K., Skene, R., Yano, J., Sang, B.C., Zou, H., Snell, G., Jennings, A., Iwamoto, K., Habuka, N., Hirokawa, A., et al. (2011). Structural analysis of the mechanism of inhibition and allosteric activation of the kinase domain of HER2 protein. J. Biol. Chem. *286*, 18756–18765.

Arkhipov, A., Shan, Y., Das, R., Endres, N.F., Eastwood, M.P., Wemmer, D.E., Kuriyan, J., and Shaw, D.E. (2013). Architecture and membrane interactions of the EGF receptor. Cell *152*, 557–569.

Binz, H.K., Amstutz, P., Kohl, A., Stumpp, M.T., Briand, C., Forrer, P., Grütter, M.G., and Plückthun, A. (2004). High-affinity binders selected from designed ankyrin repeat protein libraries. Nat. Biotechnol. *22*, 575–582.

Bocharov, E.V., Mayzel, M.L., Volynsky, P.E., Goncharuk, M.V., Ermolyuk, Y.S., Schulga, A.A., Artemenko, E.O., Efremov, R.G., and Arseniev, A.S. (2008). Spatial structure and pH-dependent conformational diversity of dimeric transmembrane domain of the receptor tyrosine kinase EphA1. J. Biol. Chem. *283*, 29385–29395.

Boersma, Y.L., and Plückthun, A. (2011). DARPins and other repeat protein scaffolds: advances in engineering and applications. Curr. Opin. Biotechnol. *22*, 849–857.

Bostrom, J., Yu, S.F., Kan, D., Appleton, B.A., Lee, C.V., Billeci, K., Man, W., Peale, F., Ross, S., Wiesmann, C., and Fuh, G. (2009). Variants of the antibody herceptin that interact with HER2 and VEGF at the antigen binding site. Science *323*, 1610–1614.

Bouyain, S., Longo, P.A., Li, S., Ferguson, K.M., and Leahy, D.J. (2005). The extracellular region of ErbB4 adopts a tethered conformation in the absence of ligand. Proc. Natl. Acad. Sci. USA *102*, 15024–15029.

Burris, H.A., 3rd, Tibbitts, J., Holden, S.N., Sliwkowski, M.X., and Lewis Phillips, G.D. (2011). Trastuzumab emtansine (T-DM1): a novel agent for targeting HER2+ breast cancer. Clin. Breast Cancer *11*, 275–282.

CCP4 (Collaborative Computational Project, Number 4). (1994). The CCP4 suite: programs for protein crystallography. Acta Crystallogr. D Biol. Crystallogr. *50*, 760–763.

Cho, H.S., and Leahy, D.J. (2002). Structure of the extracellular region of HER3 reveals an interdomain tether. Science *297*, 1330–1333.

Cho, H.S., Mason, K., Ramyar, K.X., Stanley, A.M., Gabelli, S.B., Denney, D.W., Jr., and Leahy, D.J. (2003). Structure of the extracellular region of HER2 alone and in complex with the Herceptin Fab. Nature *421*, 756–760.

Cobleigh, M.A., Vogel, C.L., Tripathy, D., Robert, N.J., Scholl, S., Fehrenbacher, L., Wolter, J.M., Paton, V., Shak, S., Lieberman, G., and Slamon, D.J. (1999). Multinational study of the efficacy and safety of humanized anti-HER2 monoclonal antibody in women who have HER2-overexpressing metastatic breast cancer that has progressed after chemotherapy for metastatic disease. J. Clin. Oncol. *17*, 2639–2648.

Craven, R.J., Lightfoot, H., and Cance, W.G. (2003). A decade of tyrosine kinases: from gene discovery to therapeutics. Surg. Oncol. *12*, 39–49.

Davis, I.W., Leaver-Fay, A., Chen, V.B., Block, J.N., Kapral, G.J., Wang, X., Murray, L.W., Arendall, W.B., 3rd, Snoeyink, J., Richardson, J.S., and Richardson, D.C. (2007). MolProbity: all-atom contacts and structure validation for proteins and nucleic acids. Nucleic Acids Res. *35*(Web Server issue), W375-83.

Dawson, J.P., Bu, Z., and Lemmon, M.A. (2007). Ligand-induced structural transitions in ErbB receptor extracellular domains. Structure *15*, 942–954.

Dreier, B., Honegger, A., Hess, C., Nagy-Davidescu, G., Mittl, P.R., Grütter, M.G., Belousova, N., Mikheeva, G., Krasnykh, V., and Plückthun, A. (2013). Development of a generic adenovirus delivery system based on structure-guided design of bispecific trimeric DARPin adapters. Proc. Natl. Acad. Sci. USA *110*, E869–E877.

Eigenbrot, C., Ultsch, M., Dubnovitsky, A., Abrahmsén, L., and Härd, T. (2010). Structural basis for high-affinity HER2 receptor binding by an engineered protein. Proc. Natl. Acad. Sci. USA *107*, 15039–15044.

Emsley, P., Lohkamp, B., Scott, W.G., and Cowtan, K. (2010). Features and development of Coot. Acta Crystallogr. D Biol. Crystallogr. *66*, 486–501.

Endres, N.F., Das, R., Smith, A.W., Arkhipov, A., Kovacs, E., Huang, Y., Pelton, J.G., Shan, Y., Shaw, D.E., Wemmer, D.E., et al. (2013). Conformational coupling across the plasma membrane in activation of the EGF receptor. Cell *152*, 543–556.

Faber, A.C., Wong, K.K., and Engelman, J.A. (2010). Differences underlying EGFR and HER2 oncogene addiction. Cell Cycle *9*, 851–852.

Ferguson, K.M., Berger, M.B., Mendrola, J.M., Cho, H.S., Leahy, D.J., and Lemmon, M.A. (2003). EGF activates its receptor by removing interactions that autoinhibit ectodomain dimerization. Mol. Cell *11*, 507–517.

Finn, R.S., and Slamon, D.J. (2003). Monoclonal antibody therapy for breast cancer: herceptin. Cancer Chemother. Biol. Response Modif. *21*, 223–233.

Fisher, R.D., Ultsch, M., Lingel, A., Schaefer, G., Shao, L., Birtalan, S., Sidhu, S.S., and Eigenbrot, C. (2010). Structure of the complex between HER2 and an antibody paratope formed by side chains from tryptophan and serine. J. Mol. Biol. *402*, 217–229.

Fitzgerald, D.J., Berger, P., Schaffitzel, C., Yamada, K., Richmond, T.J., and Berger, I. (2006). Protein complex expression by using multigene baculoviral vectors. Nat. Methods *3*, 1021–1032.

Franklin, M.C., Carey, K.D., Vajdos, F.F., Leahy, D.J., de Vos, A.M., and Sliwkowski, M.X. (2004). Insights into ErbB signaling from the structure of the ErbB2-pertuzumab complex. Cancer Cell *5*, 317–328.

Gajria, D., and Chandarlapaty, S. (2011). HER2-amplified breast cancer: mechanisms of trastuzumab resistance and novel targeted therapies. Expert Rev. Anticancer Ther. *11*, 263–275.

Garrett, T.P., McKern, N.M., Lou, M., Elleman, T.C., Adams, T.E., Lovrecz, G.O., Kofler, M., Jorissen, R.N., Nice, E.C., Burgess, A.W., and Ward, C.W. (2003). The crystal structure of a truncated ErbB2 ectodomain reveals an active conformation, poised to interact with other ErbB receptors. Mol. Cell *11*, 495–505.

Ghosh, R., Narasanna, A., Wang, S.E., Liu, S., Chakrabarty, A., Balko, J.M., González-Angulo, A.M., Mills, G.B., Penuel, E., Winslow, J., et al. (2011). Trastuzumab has preferential activity against breast cancers driven by HER2 homodimers. Cancer Res. *71*, 1871–1882.

Hollmén, M., Liu, P., Kurppa, K., Wildiers, H., Reinvall, I., Vandorpe, T., Smeets, A., Deraedt, K., Vahlberg, T., Joensuu, H., et al. (2012). Proteolytic processing of ErbB4 in breast cancer. PLoS ONE *7*, e39413.

Interlandi, G., Wetzel, S.K., Settanni, G., Plückthun, A., and Caflisch, A. (2008). Characterization and further stabilization of designed ankyrin repeat proteins by combining molecular dynamics simulations and experiments. J. Mol. Biol. *375*, 837–854.

Ishikawa, T., Seto, M., Banno, H., Kawakita, Y., Oorui, M., Taniguchi, T., Ohta, Y., Tamura, T., Nakayama, A., Miki, H., et al. (2011). Design and synthesis of novel human epidermal growth factor receptor 2 (HER2)/epidermal growth factor receptor (EGFR) dual inhibitors bearing a pyrrolo[3,2-d]pyrimidine scaffold. J. Med. Chem. *54*, 8030–8050.

Junttila, T.T., Akita, R.W., Parsons, K., Fields, C., Lewis Phillips, G.D., Friedman, L.S., Sampath, D., and Sliwkowski, M.X. (2009). Ligand-independent HER2/HER3/PI3K complex is disrupted by trastuzumab and is effectively inhibited by the PI3K inhibitor GDC-0941. Cancer Cell *15*, 429–440.

Kabsch, W. (2010). Xds. Acta Crystallogr. D Biol. Crystallogr. *66*, 125–132.

Li, S., Schmitz, K.R., Jeffrey, P.D., Wiltzius, J.J., Kussie, P., and Ferguson, K.M. (2005). Structural basis for inhibition of the epidermal growth factor receptor by cetuximab. Cancer Cell *7*, 301–311.

Liu, P., Bouyain, S., Eigenbrot, C., and Leahy, D.J. (2012). The ErbB4 extracellular region retains a tethered-like conformation in the absence of the tether. Protein Sci. *21*, 152–155.

Martin-Killias, P., Stefan, N., Rothschild, S., Plückthun, A., and Zangemeister-Wittke, U. (2011). A novel fusion toxin derived from an EpCAM-specific designed ankyrin repeat protein has potent antitumor activity. Clin. Cancer Res. *17*, 100–110.

McCoy, A.J., Grosse-Kunstleve, R.W., Adams, P.D., Winn, M.D., Storoni, L.C., and Read, R.J. (2007). Phaser crystallographic software. J. Appl. Cryst. *40*, 658–674.

Mi, L.Z., Lu, C., Li, Z., Nishida, N., Walz, T., and Springer, T.A. (2011). Simultaneous visualization of the extracellular and cytoplasmic domains of the epidermal growth factor receptor. Nat. Struct. Mol. Biol. *18*, 984–989.

Moasser, M.M. (2007). The oncogene HER2: its signaling and transforming functions and its role in human cancer pathogenesis. Oncogene *26*, 6469–6487.

Münch, R.C., Mühlebach, M.D., Schaser, T., Kneissl, S., Jost, C., Plückthun, A., Cichutek, K., and Buchholz, C.J. (2011). DARPins: an efficient targeting domain for lentiviral vectors. Mol. Ther. *19*, 686–693.

Ogiso, H., Ishitani, R., Nureki, O., Fukai, S., Yamanaka, M., Kim, J.H., Saito, K., Sakamoto, A., Inoue, M., Shirouzu, M., and Yokoyama, S. (2002). Crystal structure of the complex of human epidermal growth factor and receptor extracellular domains. Cell *110*, 775–787.

Ramamurthy, V., Krystek, S.R., Jr., Bush, A., Wei, A., Emanuel, S.L., Das Gupta, R., Janjua, A., Cheng, L., Murdock, M., Abramczyk, B., et al. (2012). Structures of adnectin/protein complexes reveal an expanded binding footprint. Structure *20*, 259–269.

Schaefer, G., Fitzpatrick, V.D., and Sliwkowski, M.X. (1997). Gamma-heregulin: a novel heregulin isoform that is an autocrine growth factor for the human breast cancer cell line, MDA-MB-175. Oncogene *15*, 1385–1394.

Sergina, N.V., Rausch, M., Wang, D., Blair, J., Hann, B., Shokat, K.M., and Moasser, M.M. (2007). Escape from HER-family tyrosine kinase inhibitor therapy by the kinase-inactive HER3. Nature *445*, 437–441.

Simon, M., Zangemeister-Wittke, U., and Plückthun, A. (2012). Facile double-functionalization of designed ankyrin repeat proteins using click and thiol chemistries. Bioconjug. Chem. *23*, 279–286.

Sliwkowski, M.X., Schaefer, G., Akita, R.W., Lofgren, J.A., Fitzpatrick, V.D., Nuijens, A., Fendly, B.M., Cerione, R.A., Vandlen, R.L., and Carraway, K.L., 3rd. (1994). Coexpression of erbB2 and erbB3 proteins reconstitutes a high affinity receptor for heregulin. J. Biol. Chem. *269*, 14661–14665.

Sliwkowski, M.X., Lofgren, J.A., Lewis, G.D., Hotaling, T.E., Fendly, B.M., and Fox, J.A. (1999). Nonclinical studies addressing the mechanism of action of trastuzumab (Herceptin). Semin. Oncol. *26*(4, Suppl 12), 60–70.

Steiner, D., Forrer, P., and Plückthun, A. (2008). Efficient selection of DARPins with sub-nanomolar affinities using SRP phage display. J. Mol. Biol. *382*, 1211–1227.

Tamaskovic, R., Simon, M., Stefan, N., Schwill, M., and Plückthun, A. (2012). Designed ankyrin repeat proteins (DARPins) from research to therapy. Methods Enzymol. *503*, 101–134.

Theurillat, J.P., Dreier, B., Nagy-Davidescu, G., Seifert, B., Behnke, S., Zürrer-Härdi, U., Ingold, F., Plückthun, A., and Moch, H. (2010). Designed ankyrin repeat proteins: a novel tool for testing epidermal growth factor receptor 2 expression in breast cancer. Mod. Pathol. *23*, 1289–1297.

Verma, S., Miles, D., Gianni, L., Krop, I.E., Welslau, M., Baselga, J., Pegram, M., Oh, D.Y., Diéras, V., Guardino, E., et al.; EMILIA Study Group. (2012). Trastuzumab emtansine for HER2-positive advanced breast cancer. N. Engl. J. Med. *367*, 1783–1791.

Webb, S.E., Roberts, S.K., Needham, S.R., Tynan, C.J., Rolfe, D.J., Winn, M.D., Clarke, D.T., Barraclough, R., and Martin-Fernandez, M.L. (2008). Single-molecule imaging and fluorescence lifetime imaging microscopy show different structures for high- and low-affinity epidermal growth factor receptors in A431 cells. Biophys. J. *94*, 803–819.

Wetzel, S.K., Ewald, C., Settanni, G., Jurt, S., Plückthun, A., and Zerbe, O. (2010). Residue-resolved stability of full-consensus ankyrin repeat proteins probed by NMR. J. Mol. Biol. *402*, 241–258.

Xia, W., Liu, L.H., Ho, P., and Spector, N.L. (2004). Truncated ErbB2 receptor (p95ErbB2) is regulated by heregulin through heterodimer formation with ErbB3 yet remains sensitive to the dual EGFR/ErbB2 kinase inhibitor GW572016. Oncogene *23*, 646–653.

Yarden, Y., and Sliwkowski, M.X. (2001). Untangling the ErbB signalling network. Nat. Rev. Mol. Cell Biol. *2*, 127–137.

Zahnd, C., Wyler, E., Schwenk, J.M., Steiner, D., Lawrence, M.C., McKern, N.M., Pecorari, F., Ward, C.W., Joos, T.O., and Plückthun, A. (2007). A designed ankyrin repeat protein evolved to picomolar affinity to Her2. J. Mol. Biol. *369*, 1015–1028.

Zahnd, C., Kawe, M., Stumpp, M.T., de Pasquale, C., Tamaskovic, R., Nagy-Davidescu, G., Dreier, B., Schibli, R., Binz, H.K., Waibel, R., and Plückthun, A. (2010). Efficient tumor targeting with high-affinity designed ankyrin repeat proteins: effects of affinity and molecular size. Cancer Res. *70*, 1595–1605.

Zhang, Q., Park, E., Kani, K., and Landgraf, R. (2012). Functional isolation of activated and unilaterally phosphorylated heterodimers of ERBB2 and ERBB3 as scaffolds in ligand-dependent signaling. Proc. Natl. Acad. Sci. USA *109*, 13237–13242.

Zhou, H., Zha, Z., Liu, Y., Zhang, H., Zhu, J., Hu, S., Shen, G., Cheng, L., Niu, L., Greene, M.I., et al. (2011). Structural insights into the down-regulation of overexpressed p185(her2/neu) protein of transformed cells by the antibody chA21. J. Biol. Chem. *286*, 31676–31683.